SPACE TELESCOPE SCIENCE INSTITUTE
Operated for NASA by AURA

Instrument Science Report ACS 2005-03

Internal monitoring of ACS charge transfer efficiency

Max Mutchler and Marco Sirianni
April 6, 2005

ABSTRACT

We present the results of over two years of inflight charge transfer efficiency (CTE) monitoring of the CCDs in the Advanced Camera for Surveys (ACS), based on two internal tests: Extended Pixel Edge Response (EPER), and First Pixel Response (FPR). In general, we find that CTE losses are worst at the lowest signal levels, and at each signal level, CTE declines linearly over time, at a rate which is consistent with results from external photometric tests (Riess, 2004). We compare our inflight results to similar pre-flight baseline data, and to predictions for inflight performance, which were based on radiation tests.

1. Introduction

Over time, the unforgiving space radiation environment wreaks havoc on flight detectors in several ways (see Janesick, 2001). For charged coupled devices (CCDs), one of the most serious effects is a gradual degradation of the charge transfer efficiency (CTE). After charge is collected in each pixel during an exposure, it is transferred down the columns of the CCD, in parallel, to the serial registers, where the charge is read out through amplifiers, one row at a time. The CTE *per pixel* is the fraction of charge transferred from one pixel to the next during this read out, which is sometimes expressed inversely as the *inefficiency*, or CTI:

$$CTE = (1 - CTI) = 1 - (\Delta Q / Q)$$

Copyright© 1999 The Association of Universities for Research in Astronomy, Inc. All Rights Reserved.

In an ideal CCD, the CTE would be exactly 1.0 -- with no charge being lost. But imperfections in the crystalline lattice of a real CCD, caused either by the manufacturing process or the space radiation environment, can act as charge traps. Although the amount of charge lost per pixel (ΔQ) is typically a very small fraction of the total charge (Q), the *total* CTE over N pixel transfers is CTE^N, which becomes increasingly significant as larger CCD arrays are manufactured and flown in space (see Hopkinson, et al., 1996).

The CCDs in the Advanced Camera for Surveys (ACS) are the two 4096 x 2048 pixel Wide Field Channel (WFC) chips, and the 1024 x 1024 pixel High Resolution Channel (HRC). They are probably among the best-studied flight detectors, in terms of the effect of radiation damage. A wealth of pre-flight CTE measurements were obtained with the flight detectors during thermal vacuum testing, and similar non-flight detectors were also tested after being artificially radiation-aged, to simulate many years of operation in low-Earth orbit (described in section 4). Since ACS was installed in the *Hubble Space Telescope* (HST) in March 2002, the CTE has continued to be monitored in several ways. External photometric tests (using the globular cluster 47 Tuc), have yielded a reliable CTE correction for ACS science data (Riess & Mack, 2004). Elevated temperature measurements have yielded some insight into the temperature dependence of CTE (Mutchler & Riess, 2004). The testing described here primarily characterizes the dependence on clocking rate (parallel versus serial clocking), signal level, and time.

Since internal tests do not involve observations of real astronomical objects -- the light source is always the internal Tungsten lamp (rather than stars) -- they do not independently lead to a CTE correction suitable for science data. But the data can be collected with great breadth and frequency (at all signal levels, throughout the life of the detector), so relative changes are therefore useful for monitoring CTE trends.

2. Internal CTE monitoring program: EPER and FPR tests

This report includes results from pre-flight thermal vacuum tests, the Servicing Mission 3B Orbital Verification (SMOV) program 8948 (PI Clampin), and the Cycle 11-13 calibration programs 9649, 10044, and 10369 (PI Mutchler). These internal monitoring programs consist of two tests performed for both the Wide Field Channel (WFC) and High Resolution Channel (HRC): **Extended Pixel Edge Response** (EPER) and the **First Pixel Response** (FPR).

Both tests produce data that are essentially flat-field frames, except they are read out with specially-designed clocking patterns, as illustrated in Figures 1-3. In the Appendix, we show how these observations are defined in a Phase II HST proposal. The impetus for conducting inflight EPER and FPR tests is described more completely in Jones et al., 1999, but we provide the following as a general summary and update.

EPER is a measurement of the excess charge found in the CCD overscans, which appears as an exponential tail following the last real pixels in the array, which tapers down to the bias level within just a few pixel transfers (see Figure 4). This tail is “deferred charge” which has been trapped during the readout, and then released on a timescale of milliseconds. EPER frames have larger overscans in the trailing directions, to accomodate the growing CTE tail while still having enough uncontaminated pixels for measurement (and subtraction) of the underlying bias level. A standard WFC frame has 4096 x 2048 pixels, with 24 physical overscans, and 20 virtual overscans. A standard HRC frame has 1024 x 1024 pixels, with 19 physical overscans, and 20 virtual overscans. Figures 1 and 3 illustrate the extra-large 75-pixel EPER overscans in the trailing directions, for WFC and HRC respectively.

While EPER measures the trailing-edge deferred charge, **FPR** measures a leading-edge loss of charge. FPR frames have a special clocking pattern where the first half of a frame is flushed (read out quickly), freshly exposing every charge trap. Then the other half of the frame is read out normally -- the electronic equivalent of a “knife-edge” test (see Figures 2 and 3). As the first column (or row) in the normal half of the chip is transferred across the flushed half, it loses charge as it fills most of the traps. We measure the charge lost in that first pixel, and compare it to the charge present in all the subsequent pixels in a column (or row), which suffer little or no charge loss. However, at the lowest signals levels, and as CTE worsens over time, we may need to measure the charge lost in the first several pixels to accurately estimate CTE (see Waczynski, et al., 2001). Note that the WFC amplifier configuration (only two amplifiers on each chip) does not allow for a parallel FPR test.

We measure the CTE in both the parallel and serial direction. The CTE is always much better in the serial direction than in the parallel direction primarily because of the faster transfer rate of the serial register: 22 µsec/pixel. For comparison, the parallel transfer rate is 3212 µsec/pixel for WFC and 1892 µsec/pixel for HRC (Sirianni et al. 2004)

With both EPER and FPR, we can measure the CTE over a wide range of signal levels. During pre-flight and SMOV testing, we sampled the full well capacity of both detectors. But in order to reduce the program’s scheduling and data volume profile, we now obtain data at fewer signal levels, and focus most of our exposure time on the lower signal levels (below 10,000 electrons), where the CTE degradation is greatest.

Every 6 months, we collect a set of EPER and FPR data over a wide range of signal levels (see Appendix). We take many more HRC exposures over a wider range of signal levels than for the WFC, because we can fit so many of these smaller frames into an orbit. We also collect a monthly “spot check”, for WFC only, at the same signal level (1620e) as the pre-flight Fe^{55} data (discussed further below). More recently, we have begun scheduling these spot checks to occur just before and after each monthly anneal, to investigate the impact of the anneal on the CTE degradation. This analysis is in progress, and the results will be presented in a separate report.

For each chip of the WFC, we repeat the tests using different amplifier pairs to reveal whether the behavior of the charge traps is dependent on the direction of the charge transfer. Our special CTE clocking patterns cannot be applied to bias frames, so we obtain short-dark “pseudo-bias” frames instead: the shortest allowable exposure time (0.5s for WFC and 0.1s for HRC, determined by the shutter speed), with the Tungsten lamp off, and the same clocking pattern as the CTE frames. We use these pseudo-bias frames to subtract bias features and fixed-pattern noise from the CTE data. In all, the internal CTE monitoring campaign consumes about 90 internal HST orbits (only during Earth occultations) per year.

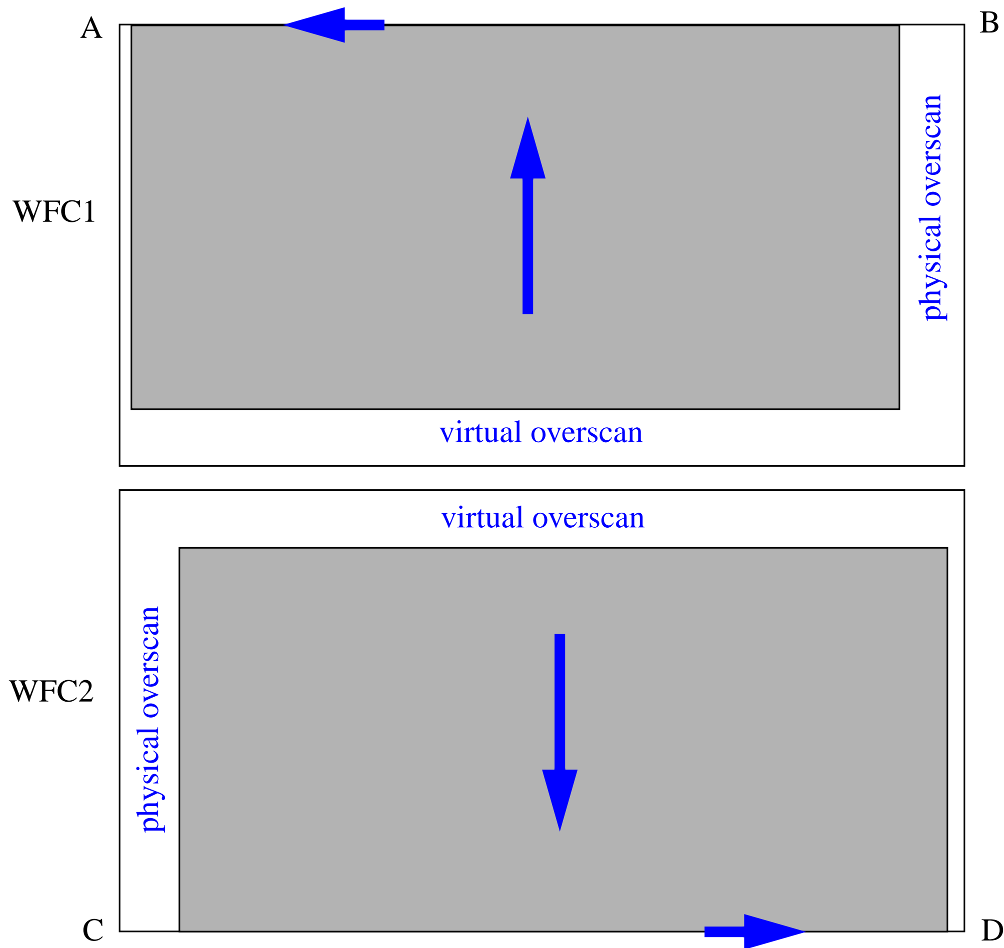

Figure 1: The WFC Extended Pixel Edge Response (EPER) test produces flats with extra-large trailing overscans (75 pixels) in both the parallel and serial clocking directions. So both parallel and serial CTE measurements can be made from each frame, for each chip. The vertical arrows indicate the parallel clocking direction, and the horizontal arrows indicate one of the serial clocking directions. The locations of the readout amplifiers (A,B,C,D) are indicated, with the amp AD readout illustrated here, while the amp BC readout is simply the mirror image.

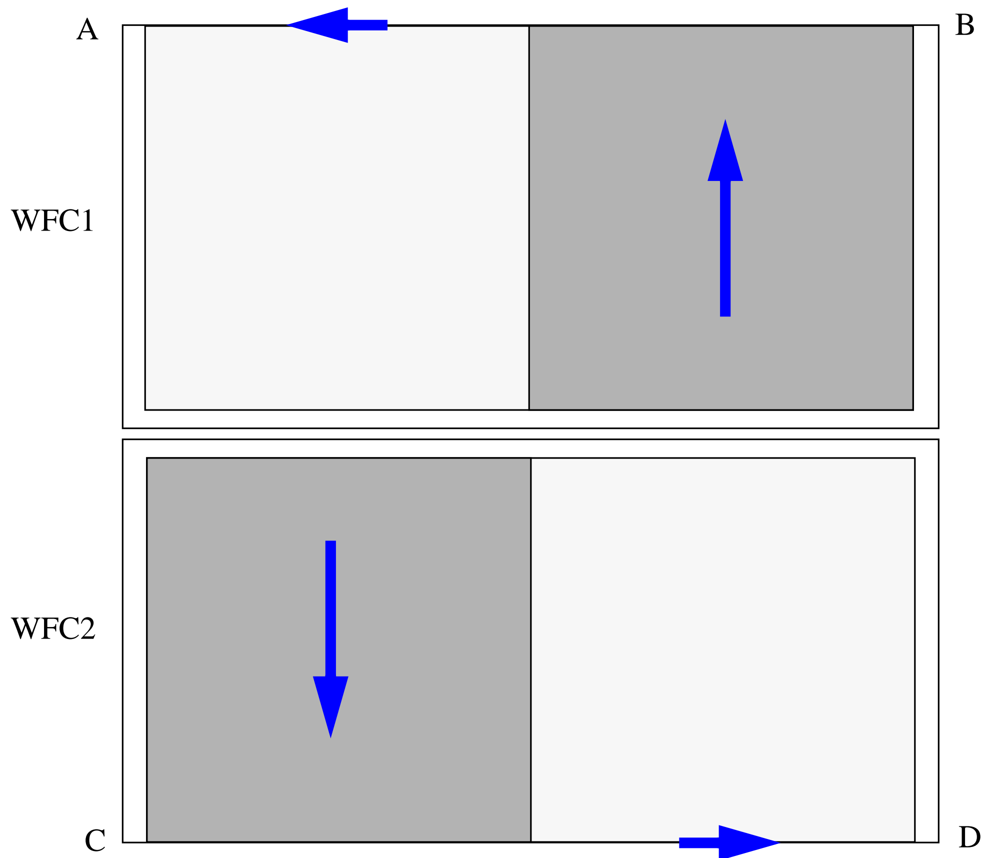

Figure 2: For the WFC, the First Pixel Response (FPR) test is limited to the serial direction due to the location of the amplifiers (A,B,C,D), with only two on each chip. One side of the chip is flushed (light gray), while the other side of the chip is read out normally (dark gray). The amp AD readout is illustrated here, while the amp BC readout is simply the mirror image. FPR data has normal-size overscans, which are used only for normal bias level subtraction.

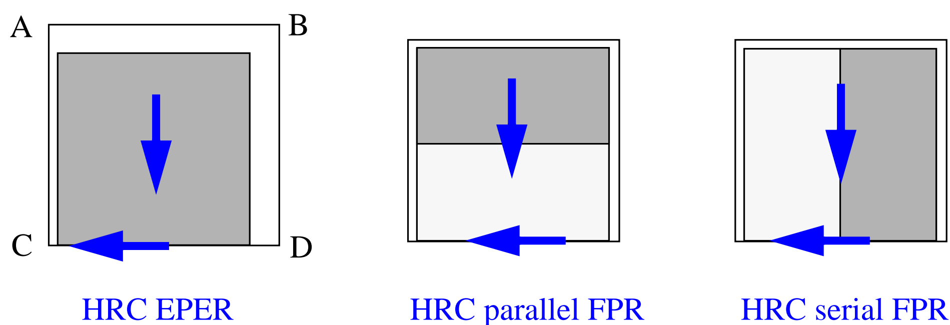

Figure 3: The HRC Extended Pixel Edge Response (EPER) test is illustrated on the left. Since the HRC has amplifiers in all four corners (A,B,C,D), the First Pixel Response (FPR) test can be performed in both the parallel (middle) and serial (right) directions. For the FPR tests, one side of the chip is flushed (fast readout; light gray above), while the other side of the chip is read out normally (dark gray above).The vertical arrows indicate the parallel clocking direction, and the horizontal arrows indicate the serial clocking direction. We now use amplifier C for all HRC tests, as illustrated above, but amp D was also used during some of the early testing (the mirror image of the graphics above).

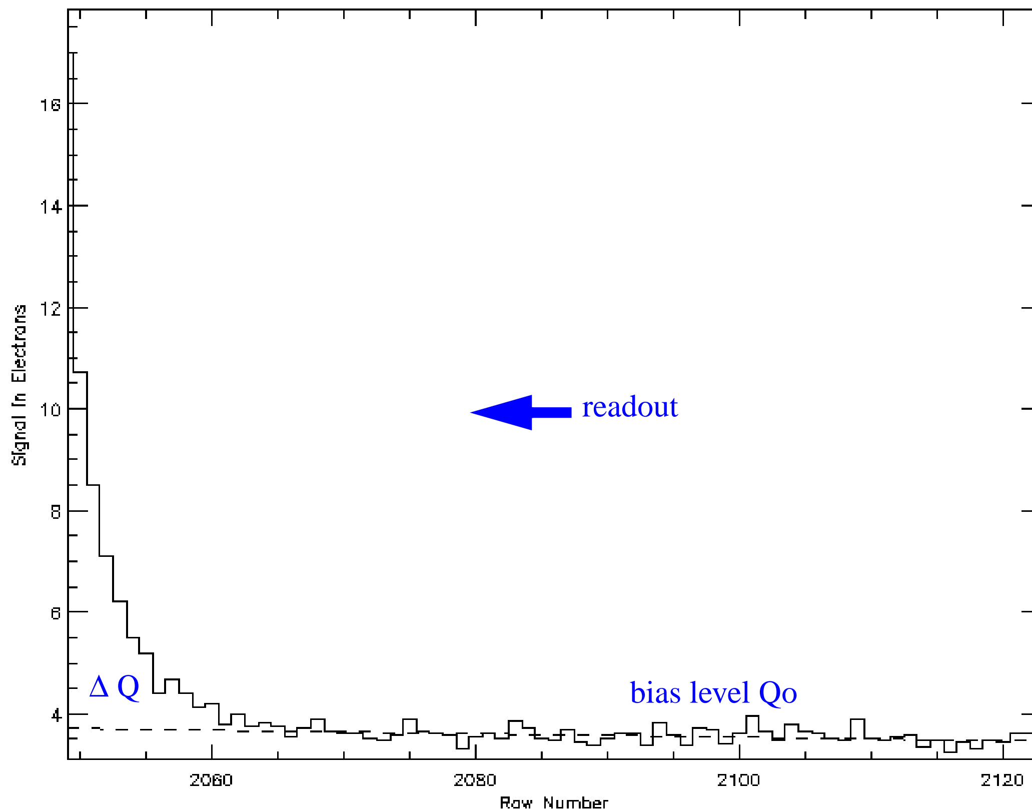

Figure 4: Extended Pixel Edge Response (EPER) measurement. This plot illustrates the parallel WFC test for the lowest signal level of ~185e, e.g. the "worst case". After subtracting the bias level (the dotted line, Q_0), the excess charge (ΔQ) in the overscan is measured, over a wide range of signal levels (Q). The y-axis represents the trailing edge (opposite the readout direction) of the detector (pixel 2048), and the x-axis shows the signal (in electrons) in the overscan. A deferred-charge tail (left) tapers off exponentially, and levels off to the underlying bias level (dotted line) within a few pixels (around overscan "pixel" 2060).

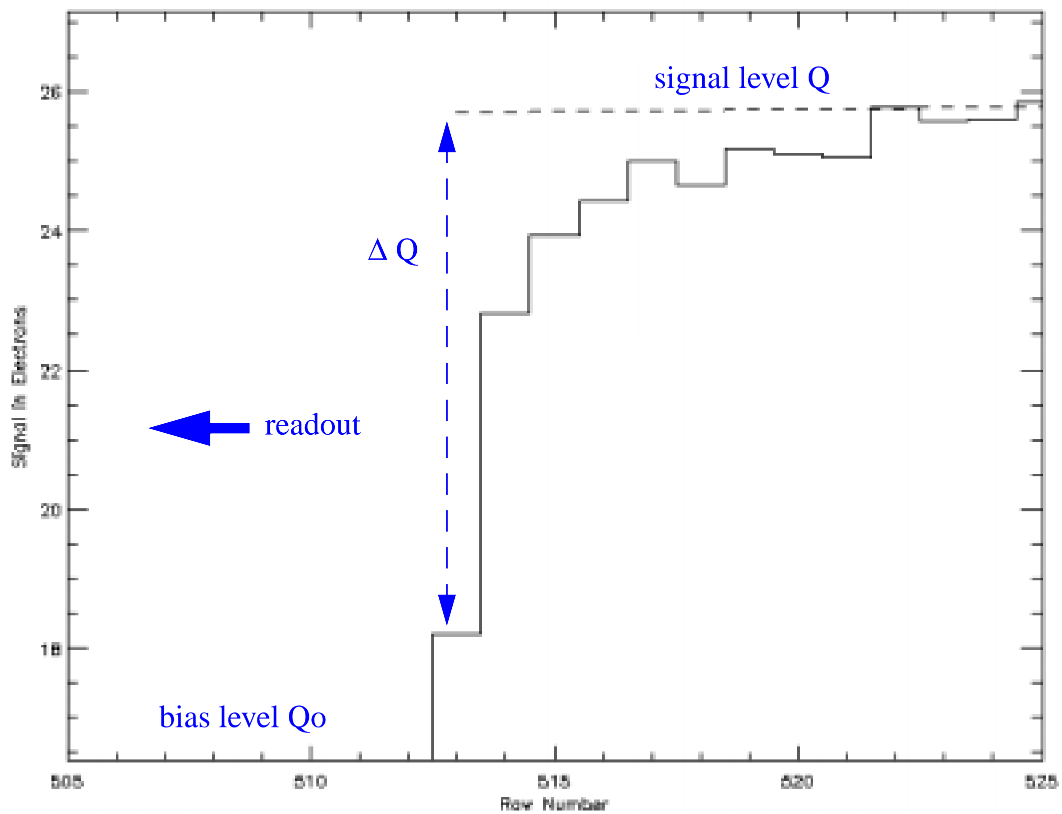

Figure 5: First Pixel Response (FPR) measurement. This plot illustrates the parallel HRC test for the lowest signal level of ~25e, e.g. the “worst case”. After subtracting the bias level (Q_0), a linear fit (dotted line) for the signal level (Q) is made. The charge lost (ΔQ) by the first pixel in each row is measured. The “first pixel” is in row 512 here, because the first half of the HRC is “flushed” (read out very fast), exposing all the charge traps. It is apparent that charge is also lost for several pixels beyond the first one, although we are not currently measuring that loss.

3. Results from inflight monitoring

The most complete and continuously updated results of our internal CTE monitoring program are maintained on the ACS website at:
http://www.stsci.edu/hst/acs/performance/cte

In this report, we highlight only the subset of data (Figures 6-10 below) which currently and most reliably illustrate our primary results:

- CTE loss is greatest at the lowest signal levels. At each epoch, the CTE exhibits a clear power law dependence on signal level (Figures 6, 9). A simple fit can therefore be used to predict CTE at any signal level with good confidence (see below).
- As expected (based on their clocking rates), parallel CTE is much worse than serial CTE for both WFC and HRC. In fact, serial CTE is still almost unmeasureably small (Figures 8, 10). A weak dependence on signal level is evident, but no trend in time can be determined, or reliably projected into the future.
- For serial FPR measurements at the lowest signal levels, we see a turnoff in our data (Figure 9): likely due to the "first-pixel" becoming less representative of the total charge lost. We exclude these points from our power law fit for now -- until we can begin including the response from subsequent pixels (see Waczynski, 2001).
- Parallel CTE degradation over time is very linear at all signal levels (Figure 7), so we can confidently model the time dependence to estimate future inflight performance.
- We see no significant difference in parallel CTE between the two WFC chips (Figure 6). These chips were cut from the same material, so we would expect they had the same initial trap population, and have degraded similarly in the space environment.
- For WFC serial CTE, we see a measureable chip dependence -- an expected result for data from the different serial registers on each chip (Figure 8, bottom)
- For HRC parallel EPER and FPR tests, we find different power laws (for the same detector, see Table 1). These tests measure different things -- charge deferred versus charge lost, respectively -- which may also be interpreted as an "optimistic" versus a "pessimistic" estimate of the same effect. But this could also be due to the HRC operating temperature of -81 C. At another operating temperature, perhaps the EPER and FPR power laws for HRC would be the same (Waczynski, 2001).

Our data consistently displays a power law function. We fit the data for each test, and for each epoch, with the following function:

$$CTE(s) = 1.0 - m*(s^p)$$

where: **s** is signal level in electrons
m is the power law multiplier
p is the power

After initially fitting each epoch independently, the average power (displayed in the header of Table 1) was calculated for each detector/test, and then the data was re-fit with the power parameter fixed. We do this on the assumption that the power law for a given chip is likely set by innate and unchanging detector characteristics (e.g. doping?). We note, however, that the power could be sensitive to the operating temperature -- which is constant for all our data. In any case, we feel that fixing the power for a given test probably leads to a more reliable fit for epochs with little data, which may become more important as we collect less data over time. Also, the fixed power law forms the basis of our extrapolations into the future (below).

Table 1. Multipliers (m) for power law fitting of parallel data from each epoch.

epoch	WFC MJD	WFC parallel EPER p=-0.61	HRC MJD	HRC parallel EPER p=-0.85	HRC parallel FPR p=-0.55
Mar 2002*	52335	0.000006	52335	0.000295	0.000252
April 2002	52375	0.000151	52375	0.000734	0.000440
Oct 2002	52554	0.000684	52554	0.001096	0.001094
April 2003	52740	0.001084	52740	0.001413	0.001664
May 2003	52764	0.001204	-	-	-
Oct 2003	52925	0.001586	52925	0.001940	0.002745
April 2004	53103	0.002099	53103	0.002615	0.003558
Oct/Nov 2004	53306	0.002635	53311	0.003101	0.004323
1 April 2005 (model)	53462	0.003040	53462	0.003512	0.005008
1 April 2006 (model)	53827	0.004007	53827	0.004501	0.006552
1 April 2007 (model)	54192	0.004974	54192	0.005490	0.008096
1 April 2008 (model)	54558	0.005944	54558	0.006482	0.009644
1 April 2009 (model)	54923	0.006912	54923	0.007471	0.011188
1 April 2010 (model)	55288	0.007879	55288	0.008461	0.012732

Based on trends in the power law fitting, a power law *model* -- CTE as a function of both signal and date - can be defined to predict future performance. Here we model only the parallel CTE:

$$CTE(s,d) = 1.0 - (n + c*(d-52335))*(s^{p})$$

where:
n is the multiplier intercept (m at launch)
c is the multiplier rate (rate of increase of m)
d is the Modified Julian Date (launch was on 1 Mar 2002 or MJD 52335)
s is the signal level in electrons
p is the power

Table 2. Coefficients for power law model, for each detector and test.

test	n	c	p
WFC parallel EPER amps ABCD	5.33e-5	2.65e-6	-0.61
HRC parallel EPER amp C	4.58e-4	2.71e-6	-0.85
HRC parallel FPR amp C	2.41e-4	4.23e-6	-0.55

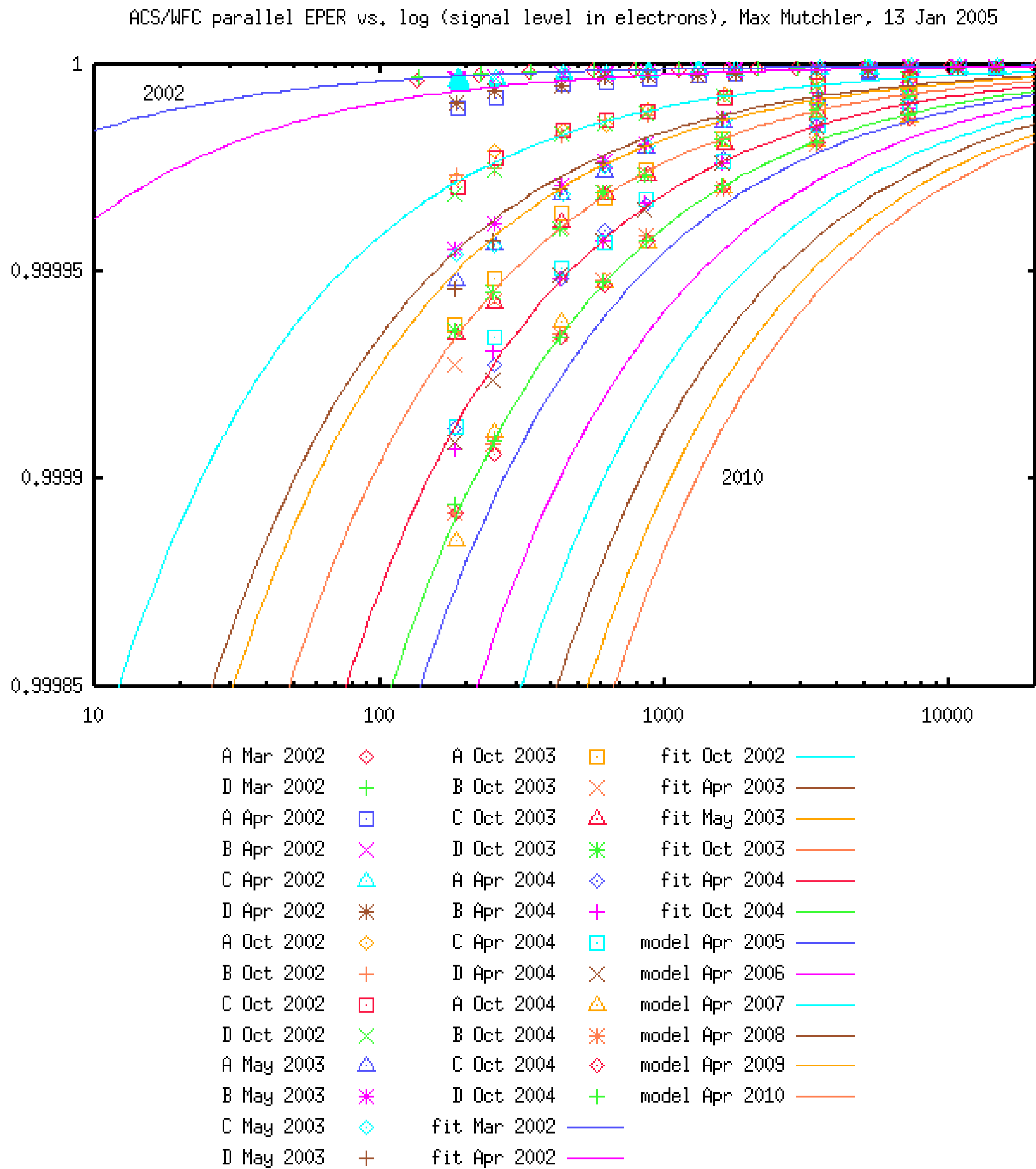

Figure 6: WFC parallel CTE as inferred from EPER data. This includes data from both chip 1 (amps A and B) and chip 2 (amps C and D). The power law fit for the data from each epoch is plotted, as is the power law model for future epochs, through 2010 (8 years in orbit).

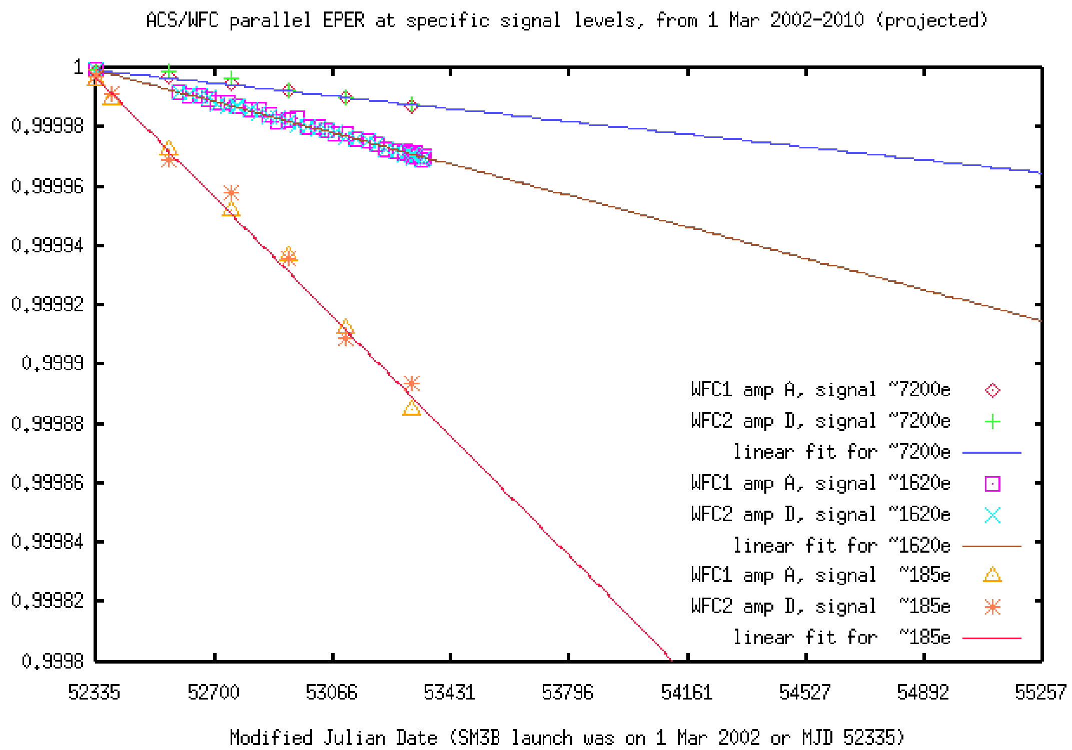

Figure 7: WFC parallel EPER at selected signal levels, over time. This plot illustrates the linearity of the CTE degradation at any given signal level, which gives us confidence in projecting our results into the future. In addition to the monthly "spot check" data at the 1620e signal level, this plot includes data points and trend lines for the lowest signal level (~185e), and a higher signal level (~7200e). The trend lines are projected out to March 2010 (MJD 55257).

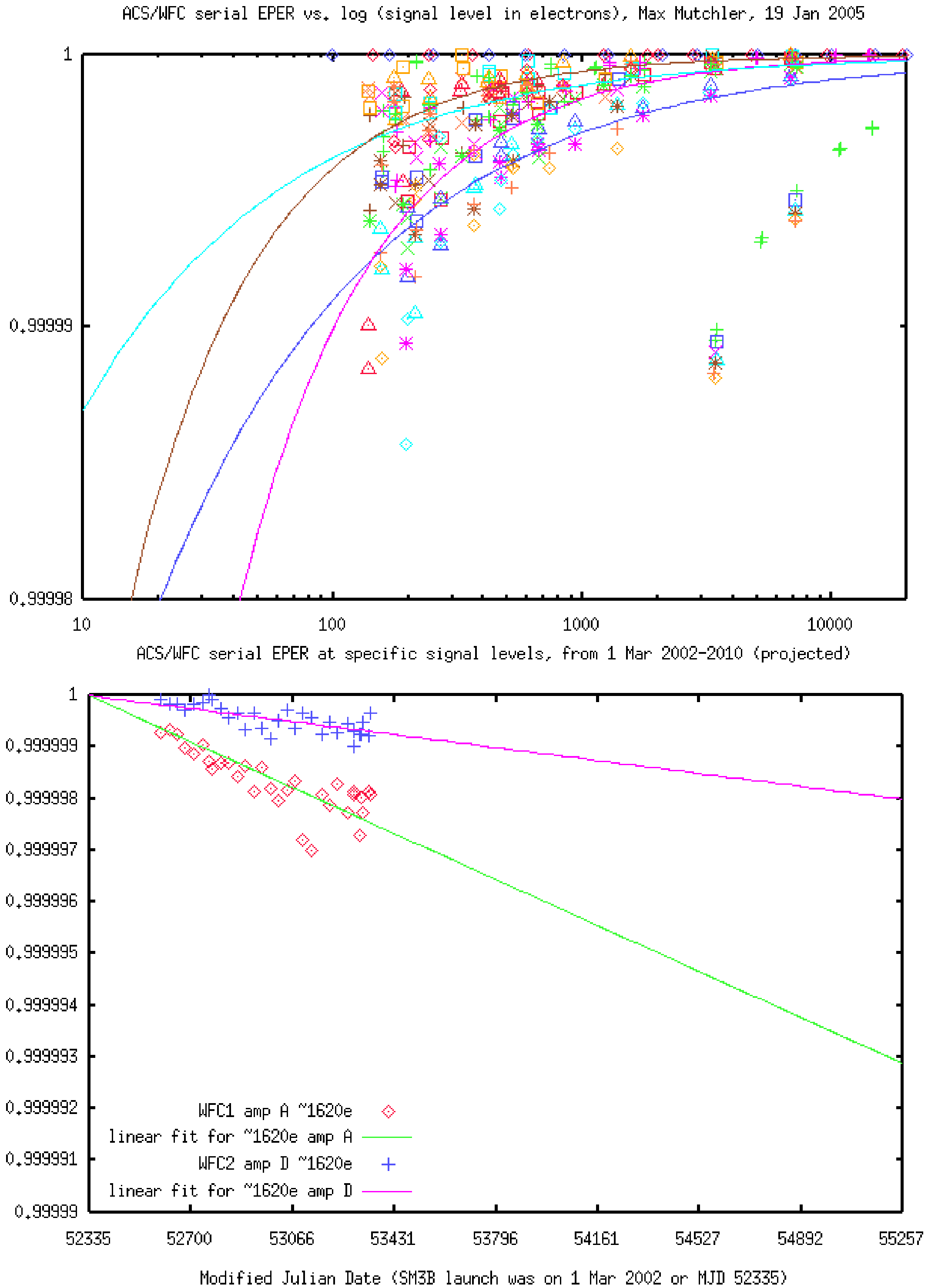

Figure 8: WFC serial CTE as inferred from EPER data. **Above:** data from all chip/amp combinations, with power law fits for each amplifier (instead of each epoch). The outlying points on the right (above ~3000e) are all from amp A, and are not understood at this point. **Below:** the chip (serial register) difference is isolated at the 1620e level (only amps AD shown here), projected out to 2010 (in MJD).

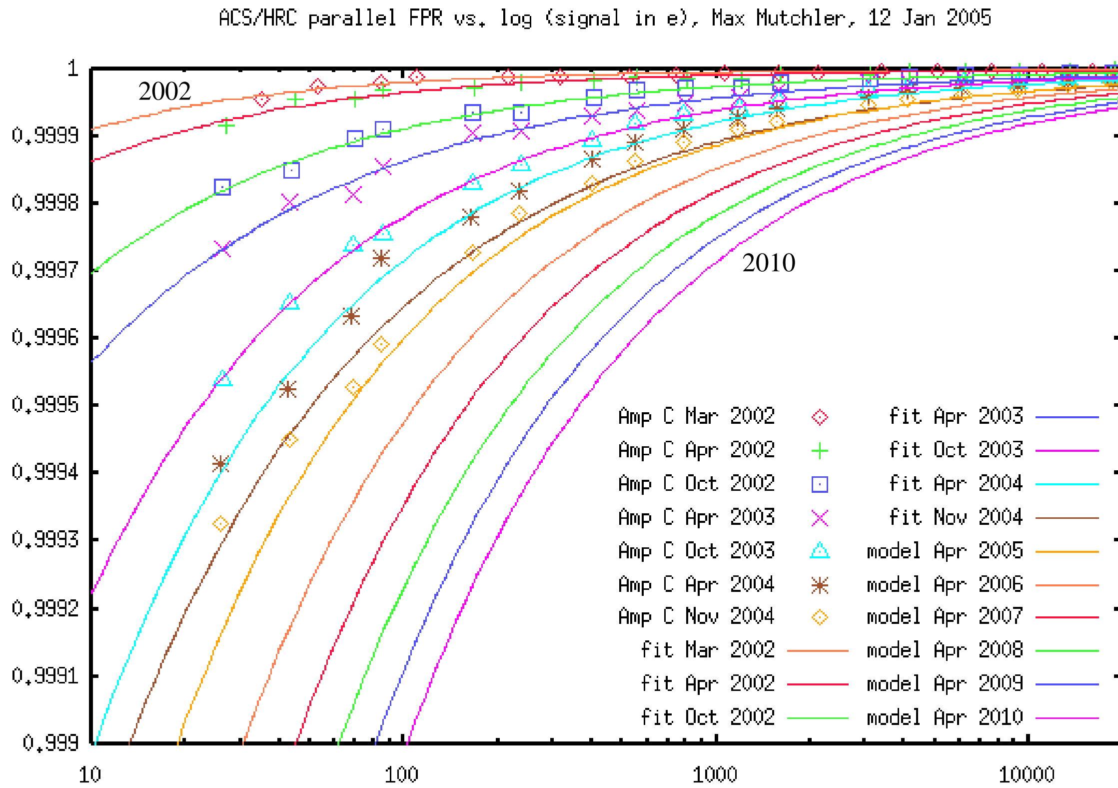

Figure 9: HRC parallel CTE, as inferred from FPR data. The dependence with signal level and the trend in time is evident.

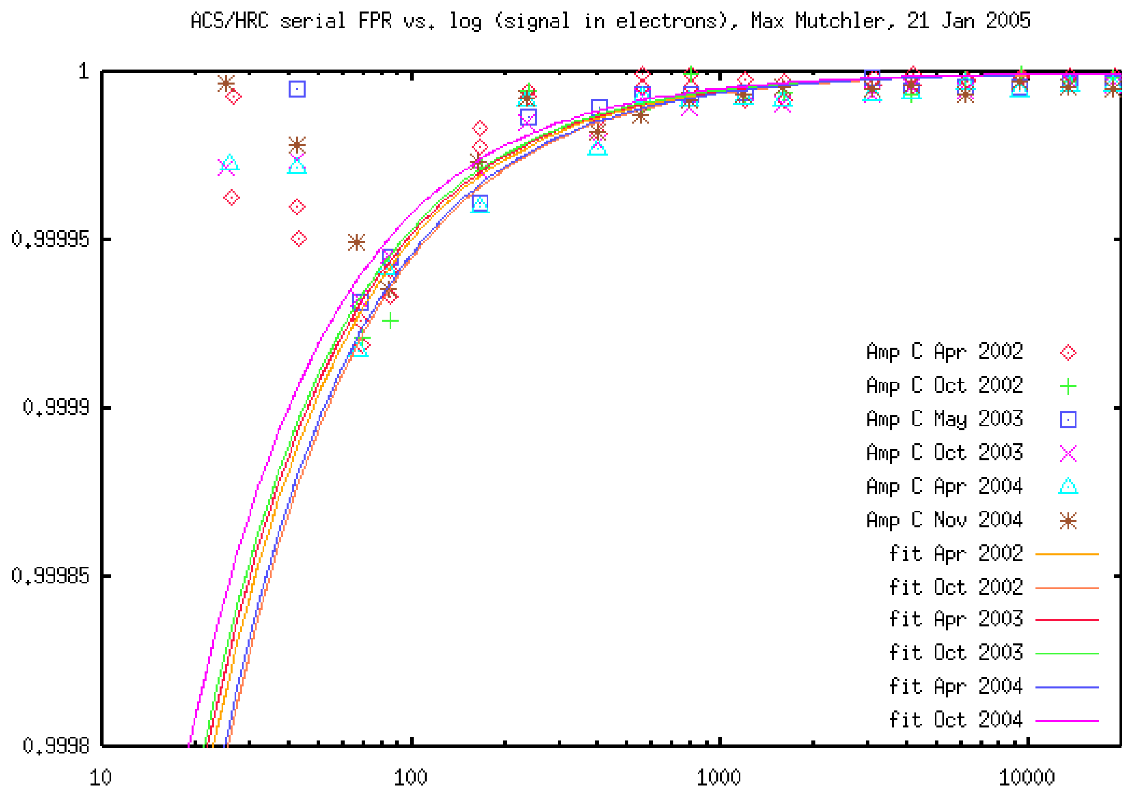

Figure 10: HRC serial CTE, as inferred from FPR data. We exclude the lowest signal level data from the power law fit, where we suspect that a significant fraction of the charge is lost beyond the first pixel (see Waczynski et al., 2001).

4. Pre-flight testing, and predictions based on radiation-aging

Two different pre-flight tests yielded results that we can compare to our inflight results. During the Thermal Vacuum 3 (TV3) campaign in July 2001 at Goddard Space Flight Center, a full complement of EPER and FPR data was obtained with ACS flight detectors in the RAS/HOMS configuration. The TV3 data points are represented in Figures 6-8 as the baseline CTE at launch (March 2002 data points). Although launch was 8 months after the TV3 tests, it is safe to assume that no additional CTE degradation occured on the ground during that interval.

In 1999, several ACS-like CCDs were bombarded with ~63 MeV protons in the Crocker Nuclear Laboratory Cyclotron at UC-Davis (Golimowski, 2000, and Jones, 2000). After the CCDs were exposed to radiation doses equivalent to 1.0, 2.5, and 5.0 years inflight operation, standard Fe^{55}, EPER, and FPR tests were conducted. Some results of this test are reprinted here, with permission from the author (Golimowski, 2000), in Figures 11 and 12. The non-flight lots 1, 5, 6B, and flight lot 7B 2K x 4K WFC chips were tested, as well as a 1K x 1K STIS flight spare, which is identical to the HRC.

The Fe^{55} is perhaps most comparable to the FPR test, in that it measures charge loss (rather than deferred charge, like the EPER test). A radioactive Fe^{55} source emits many X-rays with energy 5.89 keV, which produce charge packets that contain an average of 1620 electrons each. So each X-ray photon produces a large packet of electrons of known quantity (determined by atomic physics), and acts somewhat like a standard star that is observed simultaneously all over the CCD. By measuring the charge lost by each packet, as a function of it’s position on the chip, we get a measure of the CTE.

A “stacking plot”, like the one in Figure 11, shows the final charge measured for pixels that have undergone no transfers (left), sloping to the right for pixels that have undergone up to 2000 transfers, and everything in between. This stacking plot was produced with CCDs that were radiation-aged to a 2.5 year equivalent dose. In Figure 12, the measurements at 2.5 years are combined with the same measurements at 1.0 and 5.0 years of equivalent dose.

Comparison of results from different CTE tests with ground predictions present several difficulties. Not only do the different tests measure CTE in different ways (lost charge vs deferred charge) but also the conditions between ground testing and on-orbit operation can be different (temperature, clocking rate). Instead of using absolute CTE measurements, a comparison between different tests can be done calculating the rate of CTE degradation. Sirianni et al. (2004) have calculated the monthly CTE degradation rate for a signal of

1620e to allow a direct comparison with ground Fe^{55} tests. For the WFC parallel CTE, the EPER and external test find a degradation rate in perfect agreement ($-7x10^{-7}$). Ground testing (Fe^{55} and EPER) on radiated parts also provide a perfect agreement ($-5\ x10^{-6}$), but predict a more rapid parallel CTE degradation than observed. Similar differences are present when comparing the degradation in the serial CTE. There are several possible explanations for such differences, and more analysis is required before we can draw any firm conclusions. However it is possible, given the perfect agreement between the on-orbit tests, that the CTE degradation in ACS CCDs is proceeding slower than predicted.

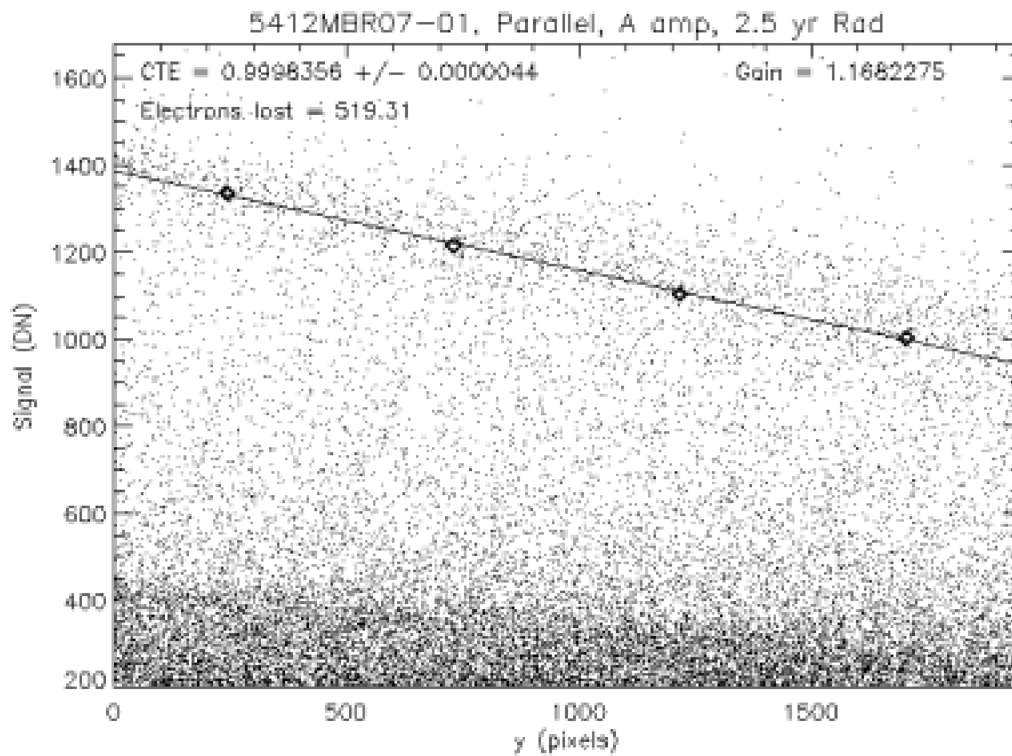

Figure 11: An Fe^{55} stacking plot for 2.5 year radiation dose for a WFC-like CCD. The initial charge of ~1620 electrons (~1400e at y=1, since gain=1.17) is depleted with increasing number of transfers. There are less than 1000 electrons left after 2000 transfers (right). Reprinted with permission from Golimowski et al. 2000.

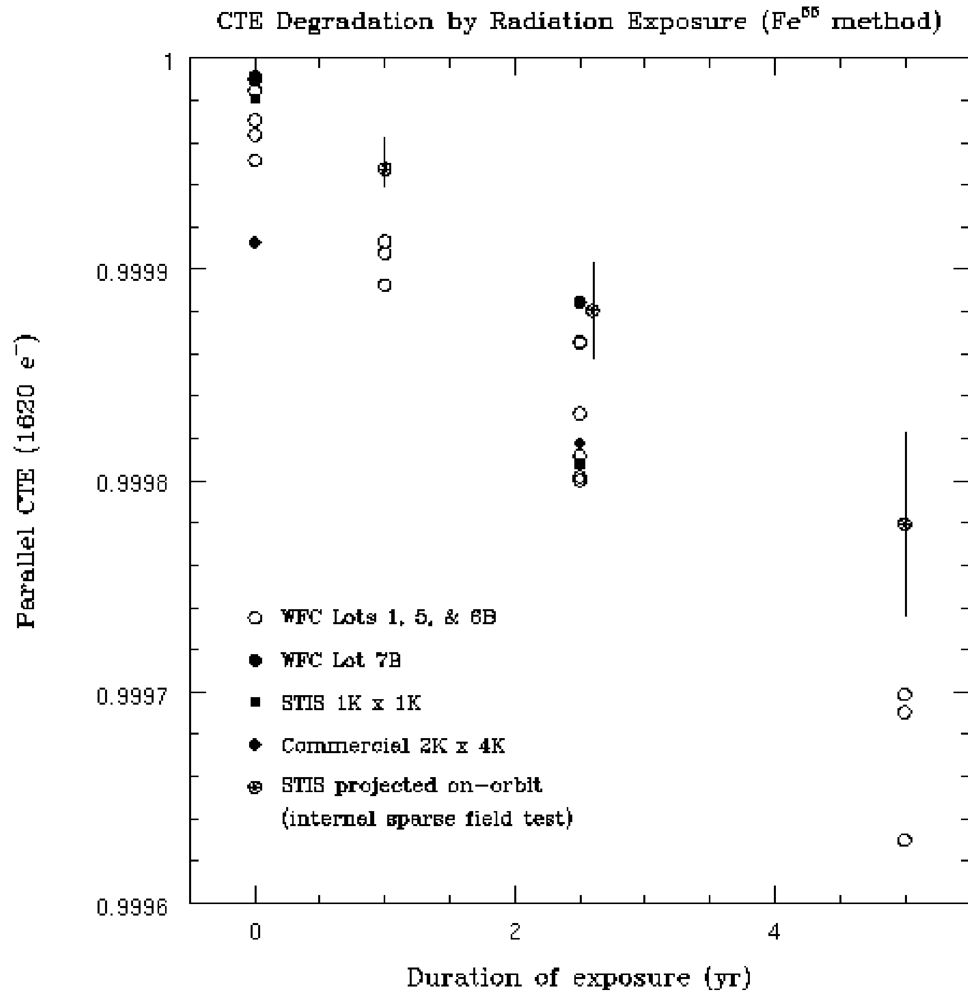

Figure 12: CTE predictions for ACS-like CCDs, based on Fe^{55} tests at 1.0, 2.5, and 5.0 year equivalent radiation doses. Reprinted with permission from Golimowski et al. 2000.

5. Summary and future work

We have independently confirmed the CTE time-dependence given in Riess, 2004. Barring the installation of an Aft Shroud Cooling System, or any other radical change to the operating temperature of these CCDs, we feel that our results can be reliably projected to the end of the Hubble mission, however soon it comes. Although we will continue to collect internal CTE data, we have no reason to believe that new data will significantly change the outlook presented here.

It is worth noting that the EPER test tends to present "optimistic" results (underestimate charge loss): perhaps more analgous to CTE loss in a science frame, where CTE is a function of sky background. Waczynski, et al., (2001) warn of the possibility that long-timescale deferred charge in the overscan could lead to an overestimate (oversubtraction) of the bias level. Further, our pre-flight testing showed that low-level flat fields (below 1000e) are affected by light leaks which depend on the shutter blade covering the detector during the readout, and the filter set in the optical path. During our SMOV program 8948, we attempted to calibrate this effect by obtaining "short-flat" pseudo-biases (with the lamp on). However, these observations failed, and were deemed infeasible. So we likely have a faint background in our CTE data which we cannot remove. Since this light leak should be constant, the relative CTE trends we are monitoring should be unaffected, but it essentially acts like a pre-flash, which effects the EPER test more than the FPR test (where the extra flux gets flushed). The FPR test tends to present "pessimistic" results: perhaps more representative of total charge loss in the detector, probably most indicative of only the "worst case" delta-magnitude in science data (which always have some sky background). Translating EPER and FPR results into a delta-magnitude correction for real objects is not straightforward, but ACS users can rely on results of the external tests (Riess, 2002) which provide a direct correction for photometric data.

On the surface, the pre-flight predictions based on Fe^{55} tests appear to differ significantly from our inflight results. But it is difficult to make precise comparisons, given the dissimilar conditions of each test. Differences could also be due to the models used to determine the radiation doses applied (to simulate inflight aging). Nonetheless, these internal CTE tests represent the best chance we have to correlate the results of the various pre-flight and inflight CTE tests -- tests done in different operational environments, with chips that have different histories, which measure different aspects of the CTE degradation, at different points in the life of the CCDs. So as we improve our ability to correlate these various results with each other, so improves our ability to use pre-flight tests to predict inflight CCD performance. As such, our internal ACS monitoring program may have it's greatest utility as a case study for the development of future flight detectors.

See our CTE website for future results from the following planned analyses:

- Compare serial amp A vs B and C vs D: do the serial registers behave the same when transferring charge in opposite directions?
- WFC serial EPER amp A (only) has a discontinuity beginning around 3300e which we don't currently understand. This is unlikely to be explained by a mini-channel effect, since we do not see the effect in the other direction (amp B).
- Problem with HRC EPER measurements: the first overscan pixel is negative. Fitting the shape of the deferred-charge tail (which will become easier as CTE worsens) would allow us to extrapolate over the "bad" pixel for a more reliable measurement.
- Problem with WFC serial FPR measurements: first pixel is too bright. Fitting the shape of the charge loss over several pixels (not just the first pixel) will allow us to extrapolate over first pixel, and measure all the lost charge (this will become easier as CTE worsens).
- Check for any dependence on CCD annealing: currently we have only a few months of 1620e data obtained just before and just after anneals.

All CTE-related documentation for ACS is maintained here, including this report, and future updates to our monitoring results:

http://www.stsci.edu/hst/acs/performance/cte

Detailed procedures for running the data reduction scripts and extracting CTE data are documented on the ACS internal website (but available from the authors upon request) primarily for use by the ACS group:

http://www.stsci.edu/hst/acs/team/procedures

Acknowledgements

We thank Mike Jones for essential contributions to all phases of this monitoring program: developing the special clocking patterns (see Appendix, Table 3), designing the initial observing strategy and Phase II proposals, and writing the initial IDL analysis code. Thanks to Alan Welty for his role in developing and implementing the internal CTE clocking patterns that make this monitoring program possible. Thanks also to to our Program Coordinator Alison Vick for helpful implementation advice and observation scheduling.

References

Ford, Golimowski, Tsvetanov, & Clampin, 2000, “Radiation damage and preflash remediation”, white paper
http://www.stsci.edu/hst/acs/performance/cte_workgroup/papers/ford_wp.pdf

Golimowski, 2000, “CTE degradation of ACS CCDs in a simulated HST radiation environment”, *STScI CTE Workshop*
http://www.stsci.edu/hst/acs/performance/cte_workgroup/papers/golimowski.pdf

Hopkinson, Dale, & Marshall, 1996, “Proton effects in CCDs”,
IEEE Trans. Nucl. Sci., vol. 43

Janesick, 2001, "Scientific Charged-Coupled Devices", *SPIE Press Monograph* PM83

Jones, 2000, “ACS WFC CCD radiation test: the radiation environment”,
ACS Instrument Science Report 00-09
http://www.stsci.edu/hst/acs/documents/isrs/isr0009.pdf

Jones, Clampin, Meurer, & Schrein, 1999, “Justification and requirements for on-board ACS FPR/EPER CTE calibration”, *ACS Technical Instrument Report 99-03*
http://www.stsci.edu/hst/acs/documents/isrs/isr9903.pdf

Mutchler & Riess, 2004, “Elevated temperature measurements of ACS CTE”,
ACS Instrument Science Report 04-04
http://www.stsci.edu/hst/acs/documents/isrs/isr0404.pdf

Riess & Mack, 2004, “Time Dependence of ACS WFC CTE Corrections for Photometry and Future Predictions”, *ACS Instrument Science Report 04-06*
http://www.stsci.edu/hst/acs/documents/isrs/isr0406.pdf

Sirianni, Mutchler, Clampin, Ford, Illingworth, Hartig, van Orsow, & Wheeler, 2004, “Performance of the ACS CCDs After Two Years on Orbit”, *Proc. SPIE* vol. 5499
http://acs.pha.jhu.edu/instrument/papers/documents/sirianniSPIE04.pdf

Waczynski et al. 2001, “A Comparison of CTE measurement techniques on proton damaged n-channel CCDs for the HST Wide-Field Camera 3”, *IEEE Transactions on Nuclear Science*, vol. 48, no. 6, 1807

Appendix: Internal CTE monitoring exposures

Special commanding is required to execute internal CTE exposures. The EPER and FPR clocking patterns described above, are invoked in a Phase II Proposal with the following Optional Parameters. Only the clocking patterns used in our monitoring programs are listed here, although patterns for other detector/amplifier combinations are also available.

Table 3. Optional Parameters for specifying internal CTE exposures in an HST proposal.

Optional Parameters	Description
CTE=JCTWE, AMP=AD	WFC parallel and serial EPER test with amps AD.
CTE=JCTWE, AMP=BC	WFC parallel and serial EPER test with amps BC.
CTE=JCTWFS, AMP=AD	WFC serial FPR test with amps AD.
CTE=JCTWFS, AMP=BC	WFC serial FPR test with amps BC.
CTE=JCTHE, AMP=C	HRC parallel and serial EPER test with amp C.
CTE=JCTHFP, AMP=C	HRC parallel FPR test with amp C.
CTE=JCTHFS, AMP=C	HRC serial FPR test with amp C.

Tables 3 and 4 show the filters and exposure times used to generate the range of signal levels for the WFC and HRC internal CTE tests. Crossed filters are used to generate the lowest signal levels. The lowest signal level is limited by the lowest legal exposure times (0.5 sec for WFC, and 0.1 sec for HRC), which in turn are limited by the shutter speeds.

Table 4. WFC filters and exposure times for internal CTE monitoring program.

WFC Filters	Exposure time	Intended signal level	Measured signal level
F555W, F435W	0.5 s	125 e	180e
F555W, F435W	0.7 s	300 e	250e
F555W, F435W	1.2 s	500 e	430e
F555W, F435W	1.7 s	700 e	610e
F555W, F435W	2.4 s	1,000 e	850e
F555W, F435W	4.5 s	1,620 e	1600e
F435W	1.0 s	5,000 e	3400e
F435W	2.1 s	10,000 e	7200e
F435W	6.3 s	30,000e	21,500e

Table 5. HRC filters and exposure times for internal CTE monitoring program.

HRC Filters	Exposure time	Intended signal level	Measured signal level
F502N	0.3 s	30 e	25e
F502N	0.5 s	50 e	43e
F502N	0.8 s	75 e	68e
F502N	1.0 s	100 e	84e
F502N	2.0 s	200 e	164e
F502N	2.9 s	300 e	235e
F502N	4.9 s	500 e	398e
F502N	6.8 s	700 e	547e
F502N	9.8 s	1,000 e	782e
F502N	14.7 s	1,500 e	1176e
F502N	19.6 s	2,000 e	1570e
F625W	0.3 s	3,000 e	3070e
F625W	0.4 s	5,000 e	4100e
F625W	0.6 s	7,000 e	6200e
F625W	0.9 s	10,000 e	9200e
F625W	1.3 s	15,000 e	13,300e
F625W	1.8 s	20,000 e	18,400e
F625W	2.7 s	30,000 e	27,700e
F625W	4.4 s	50,000e	45,100e
F625W	6.2 s	70,000e	63,400e
F625W	7.9 s	90,000e	80,700e
F625W	10.5 s	120,000e	107,300e